



Effects of under-aging treatment on microstructure and mechanical properties of squeeze-cast Al–Zn–Mg–Cu alloy

Fei-fan WANG^{1,2}, Wen MENG^{1,2}, Hong-wei ZHANG¹, Zhi-qiang HAN^{1,2}

1. School of Materials Science and Engineering, Tsinghua University, Beijing 100084, China;

2. Key Laboratory for Advanced Materials Processing Technology, Ministry of Education, Tsinghua University, Beijing 100084, China

Received 31 July 2017; accepted 15 January 2018

Abstract: The effects of under-aging treatment on the microstructure and mechanical properties of Al–Zn–Mg–Cu alloy produced by squeeze casting were investigated using optical microscopy (OM), X-ray diffractometry (XRD), scanning electron microscopy (SEM), transmission electron microscopy (TEM) and hardness and tensile testing. The results showed that most of secondary phases were dissolved into α (Al) matrix while no significant grain growth happened under the condition of solution treatment at 470 °C for 4 h. Due to the strengthening effect of GP zones, for alloys treated by under-aging process, the increase of aging time and aging temperature improved the ultimate tensile strength (UTS) and yield strength (YS), but decreased the elongation (δ) to some extent. By utilizing appropriate aging time and temperature, the best combination of strength and ductility could be obtained to fulfill the design requirements of automobile components.

Key words: Al–Zn–Mg–Cu alloy; squeeze casting; under-aging treatment; GP zone; precipitation strengthening

1 Introduction

In recent years, the retaining number of automobiles has been increasing steadily, which has impacted the natural environment significantly [1]. As a consequence of a growing car market, the using of automobiles accounts for almost one third of CO₂ emissions in the world [2]. These may lead to many severe environment problems. A rough estimate suggests that a mass reduction of 100 kg of automobiles results in decreased fuel consumption of 5%. A rule of thumb is that a 10% mass reduction results in a 4%–6% decrease in fuel consumption, indicating some of the potential in focusing on lightmass concepts in the automotive industry [3]. One of the important methods to reduce the automobile mass is the use of lightmass materials such as aluminum and magnesium alloys [4].

Aluminum alloys based on Al–Zn–Mg–Cu system in virtue of their attractive properties of lightmass and high strength are widely used in transportation applications where they are subjected to demanding operating conditions [5]. Al–Zn–Mg–Cu wrought alloys were commonly formed by wrought manufacture process

such as equal-channel angular pressing (ECAP), severe plastic deformation (SPD), cryo-rolling, or other controlled thermo-mechanical treatment (TMT), which resulted in especially excellent mechanical properties [6,7]. However, the cost of this production route is very high compared with the alternative casting route. In fact, the requirement of mechanical properties of automobile components varies from case to case. There is no need to achieve the best mechanical performance in all aspects which may make a big increase in cost. Taking control arm as an example, the design requirement of its ductile is very high, while relatively good yield strength (YS) and ultimate tensile strength (UTS) can meet the design requirement. Thus, a manufacture process which is not only economical, but also can produce components that meet the design requirements is needed.

In contrast to wrought manufacture process, casting is an economic fabrication method. However, due to the poor fluidity of high strength Al–Zn–Mg–Cu alloys, defects such as micro-pores and shrinkage cavities are found in products manufactured by conventional casting process [8]. For squeeze casting process, molten metal was solidified under high applied pressure. The high

pressure used in this process, leads to excellent feeding of solidification shrinkage and a refined microstructure, both of which result in excellent mechanical properties [9]. In addition, squeeze-cast components also show improved response to heat treatment. However, there have been only scattered reports on these processes of squeeze-cast Al–Zn–Mg–Cu alloys. Many articles focused on process parameters such as applied pressure and pouring temperature. For example, KIM et al [10] investigated the properties of the direct squeeze-cast 7075 wrought Al alloy produced under different pressures. The effects of the casting temperatures on the microstructure and mechanical properties of squeeze-cast Al–Zn–Mg–Cu alloys were investigated by FAN et al [11].

Heat treatment process has a great influence on the microstructure and properties of Al–Zn–Mg–Cu alloys. In order to achieve required properties, various artificial aging treatments, such as under-aging, peak-aging, over-aging, multistage-aging, are widely used [12]. The peak-aged alloys have high strength, whereas under-aged alloys provide good ductility. Multistage-aging processes are often adopted to further improve the mechanical properties and corrosion resistance of Al–Zn–Mg–Cu alloys [13,14]. For the application of Al–Zn–Mg–Cu alloy in producing automobile components, the combination of excellent strength and good ductility is an important issue. Under-aging and multistage-aging are proper candidate processes to achieve this goal. However, aging processes such as multistage-aging are often complicated. In contrast, the short aging time of under-aging process will improve the production efficiency, which is conducive to the further application of the alloys. However, systematical studies on the microstructure and properties of under-aging process of squeeze-cast Al–Zn–Mg–Cu alloys have rarely been reported.

The objectives of the present study are to investigate the effects of parameters of under-aging treatment on the microstructure and mechanical properties of squeeze-cast Al–Zn–Mg–Cu alloys, and to obtain the best combination of strength and ductility which can fulfill the design requirements of automobile components.

2 Experimental

The Al–Zn–Mg–Cu alloy with the chemical compositions listed in Table 1 was chosen for the present study. In the experiments, direct squeeze casting was adopted. The pouring temperature and the applied pressure were 700 °C and 120 MPa, respectively. The dimensions of the casting ingots were 120 mm × 60 mm × 40 mm. Test specimens were cut from the

ingots for microstructural examination, hardness measurements and tensile testing.

In order to study the solution process, specimens were solution-treated at 470 °C for 2, 3, 4 and 5 h and subsequently quenched into cold water. Specimens for studying aging process were solution-treated by the selected optimal process and aged under various conditions. The aging temperatures were 105, 120 and 135 °C and the aging time was 2, 4, 6 and 8 h.

Table 1 Chemical composition of Al–Zn–Mg–Cu alloy (mass fraction, %)

Zn	Mg	Cu	Fe	Si	Al
4.91	1.99	1.5	0.42	0.19	Bal.

The microstructures of the samples were characterized by optical microscope (OM) and JEM2010 transmission electron microscope (TEM). The grain sizes were measured according to the ASTM Standard E112. Hardness (HV) measurements to figure out the age-hardening behavior were performed using a HV–5 hardness tester with a load of 50 N for 15 s. Five hardness measurements were taken for each sample, and the average value was adopted. The flat dog-bone tensile specimens with a gauge length of 30 mm and a cross-section of 6 mm × 3 mm (18 mm²) were cut from the squeeze-cast ingots by using an electric-spark wire-cutting machine. Tensile testing was conducted at room temperature on a universal testing machine with the strain rate of 1.5 mm/min. For each condition, 3–8 tensile tests were performed. The fracture of tensile samples was analyzed by a ZEISS Merlin field emission scanning electron microscope (SEM). The phase identification was performed by a D/max2500HB+/PC X-ray diffractometer (XRD) with a scanning speed of 2 (°)/min.

3 Results and discussion

3.1 Effects of solution process

Solution treatment is an important part of heat treatment. It is carried out at a relatively high temperature to dissolve the secondary phases formed during solidification to achieve a high and homogeneous concentration of the alloying elements in solid solution. Then, quenching, usually to room temperature, to obtain a supersaturated solid solution of solute atoms and vacancies, is very important for age hardening. However, long time of solution treatment will lead to additional growth of grains, which induced poor mechanical properties of alloys. It is reported that the secondary phases disappear after 24 h homogenization at 460 °C [15], which seems to be too long for squeeze-

cast products and will lead to additional grain growth. Therefore, experiments need to be carried out to find the optimal solution treatment temperature and time.

Figure 1 shows the microstructures of as-cast Al–Zn–Mg–Cu alloy composed of $\alpha(\text{Al})$ grains with dendrite character and secondary phases. Figure 2 shows the optical micrographs of alloys solution-treated at 470 °C for different time. The volume fraction of the secondary phase was analyzed and calculated based on the quantitative metallographic analysis using Image-Pro (image analysis software). With the increase of solution treatment time, the volume fraction of secondary phase decreased, and the average grain size increased, as shown in Table 2. After 4 h of solution treatment, the secondary phases were almost completely dissolved into the $\alpha(\text{Al})$ matrix, and only very small amount of “black line” phases remained along the grain boundaries. When solution treatment time was increased from 4 to 5 h, the

volume fraction of secondary phases was almost unchanged and the average grain size increased sharply as shown in Table 2. Therefore, taking into account the degree of dissolution of secondary phases and the grain growth, the optimal solution process was treating at 470 °C for 4 h. As shown in Fig. 3, the XRD spectra showed similar result. The as-cast alloy was mainly composed of $\alpha(\text{Al})$ and MgZn_2 (known as η phase). MgZn_2 is the main component of secondary phases. After the solution treatment of the as-cast alloys, the peaks of MgZn_2 become invisible, which demonstrated that the secondary phase has dissolved into $\alpha(\text{Al})$ matrix. It is noted that other secondary phases including S (Al_2CuMg), T ($\text{Mg}_3\text{Zn}_3\text{Al}_2$), $\text{Al}_7\text{Cu}_2\text{Fe}$ and Mg_2Si phases [16] were difficult to be dissolved into $\alpha(\text{Al})$ matrix and remained along grain boundaries after 4 h of solution treatment at 470 °C. Due to the relatively small amount, the XRD peaks of those phases were not found.

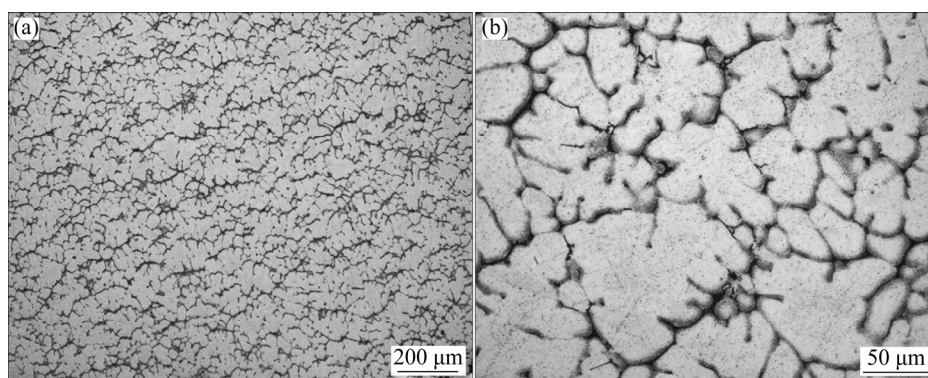


Fig. 1 Microstructures of as-cast alloys: (a) Overall morphology; (b) Local morphology

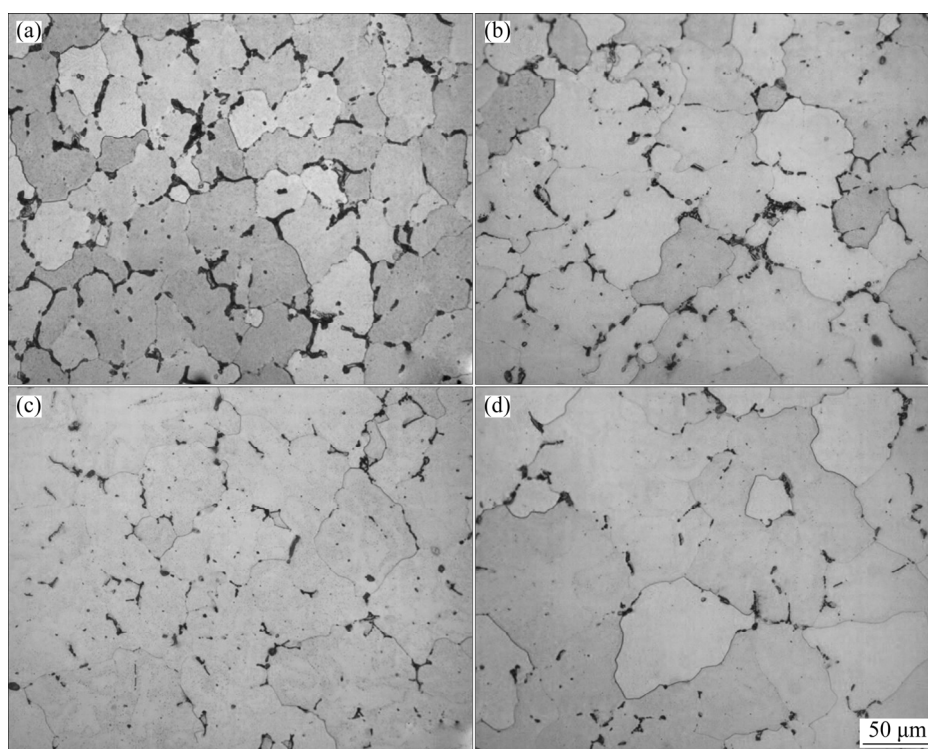
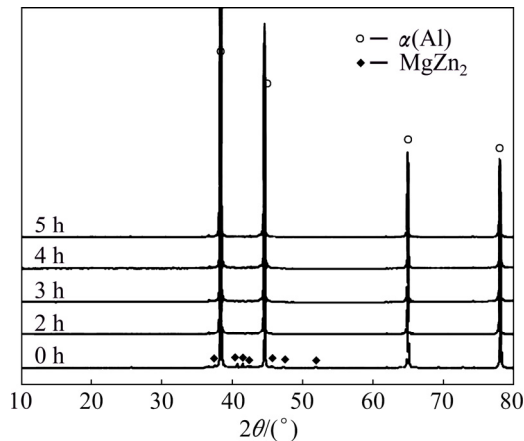


Fig. 2 Microstructures of alloys solution-treated at 470 °C for different time: (a) 2 h; (b) 3 h; (c) 4 h; (d) 5 h

Table 2 Volume fractions of secondary phases and average grain size of samples solution-treated at 470 °C for different time

Solution treatment time/h	Average grain size/ μm	Volume fraction of secondary phases/%
2	54.90	7.43 \pm 0.72
3	68.27	6.01 \pm 0.56
4	77.04	5.01 \pm 0.69
5	105.80	4.40 \pm 0.43

**Fig. 3** XRD patterns of as-cast and solution-treated alloys

The solution treatment process involved the change of mechanical properties of alloys. The tensile properties of the as-cast and solution-treated alloys were provided in Table 3. The results showed that there is no obvious change in the value of UTS. The value of YS was dropped by 40.3% after solution treatment, from 220.94 to 132.50 MPa. The δ value of the as-cast alloy is only 2.32%, while that of the solution-treated alloy is 16.44%.

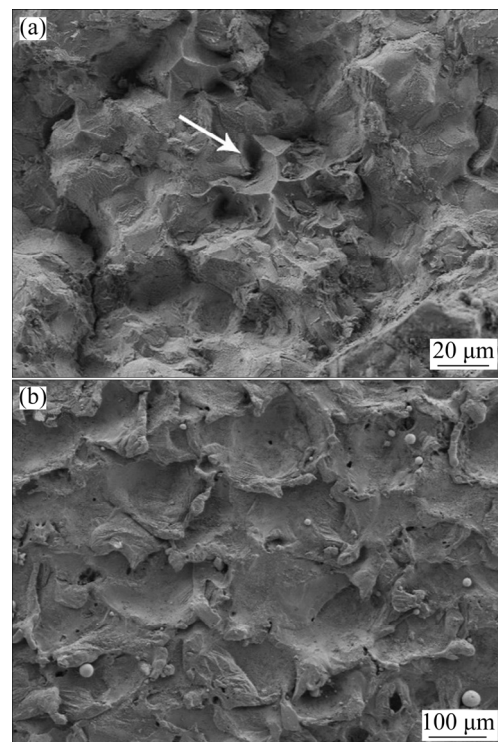
Table 3 Tensile properties of as-cast and solution-treated alloys

Alloy state	UTS/MPa	YS/MPa	δ /%
As-cast	297.23 \pm 17.25	220.94 \pm 23.60	2.23 \pm 0.69
Solution-treated for 4 h	300.54 \pm 16.82	132.50 \pm 6.50	16.44 \pm 3.56

For as-cast alloy, secondary phases were distributed along grain boundaries. On the one hand, these secondary phases can block dislocations across adjacent grain boundaries. Thus, the YS of the material was improved. On the other hand, the poor deformation ability of secondary phases induced stress concentration. As a result, the fracture sources formed at grain boundaries. Therefore, the ductility of the material deteriorated. After solution treatment at 470 °C for 4 h, the volume fraction of secondary phases was greatly reduced, and the strengthening effect of secondary phases at grain boundaries was weakened. At the same time, the solute atoms were dissolved into the $\alpha(\text{Al})$

grains, which caused lattice distortion and resulted in a solid solution strengthening effect. The results of the present study showed that the solid solution strengthening effect was insufficient to compensate for the weakening of the secondary phases strengthening effect. As a result, the yield strength of the solution-treated alloy decreased dramatically compared with the as-cast alloy. Besides, due to the decrease of the volume fraction of secondary phases along grain boundaries, it was easier for the dislocations to travel from one grain to the next instead of forming dislocation pile-ups against grain boundaries, and deformation coordination ability of different grains was greatly improved. As a result, the ductility of the solution-treated alloy is greatly increased.

The fracture morphologies of as-cast and solution-treated alloys are shown in Fig. 4. The as-cast alloy showed a candy-like intergranular fracture feature, as shown in Fig. 4(a), while the solution-treated alloy exhibited the ripple-like pure shear fracture morphology in Fig. 4(b). The reason for intergranular fracture feature of as-cast alloy was the crack sources along grain boundaries, which resulted from the dislocation accumulation and brittle secondary phases. For solution-treated alloy, most of the secondary phases were dissolved into $\alpha(\text{Al})$ grain matrix, and the ductility of the alloy was greatly improved, as shown in Table 3. Therefore, a ripple-like pure shear fracture morphology was observed in solution-treated alloy.

**Fig. 4** Fracture morphologies of as-cast and solution-treated alloys: (a) As-cast alloy; (b) Alloy solution-treated at 470 °C for 4 h

The experiment results in the present study showed that most of secondary phases were dissolved into the $\alpha(\text{Al})$ grains after 4 h of solution treatment at 470 °C without obvious grains growth. The purpose of solid solution treatment has been achieved. Therefore, the alloys were solution-treated at 470 °C for 4 h followed by water quenching before under-aging process.

3.2 Effects of aging conditions

During the aging process, supersaturated Al solid solution decomposes, precipitation occurs, and the strength of the alloys increases. The precipitation sequence of Al–Zn–Mg–Cu alloys is as follows: supersaturated solid solution (SSS) \rightarrow coherent GP zones $\rightarrow \eta'$ phase (semi-coherent precipitates) \rightarrow stable precipitates [17,18].

Figure 5 shows the TEM images of the microstructure of under-aged alloys, in which small circular GP zones can be observed on the matrix. Metastable η' phase and stable phase η , which were often flaky or strip, were not found. The diameter of the GP zone was 2–3 nm, and the alloy aged at 120 °C for 4 h had a less fraction of GP zone than that aged at 120 °C for 8 h. The fraction of GP zones increased with the increase of aging time.

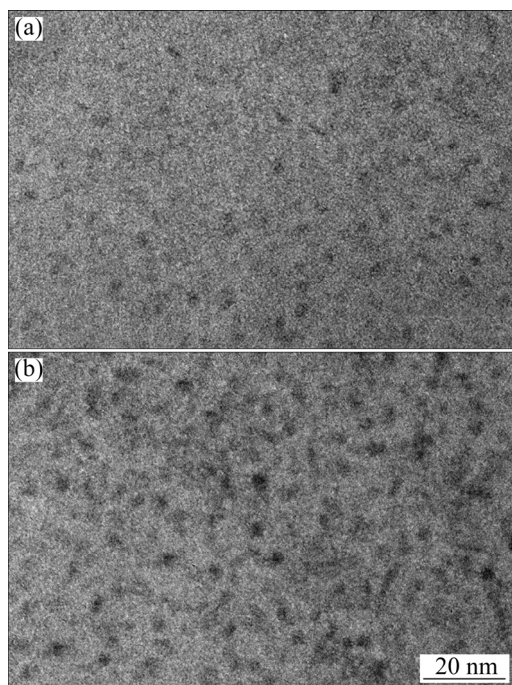


Fig. 5 TEM images of alloys under-aged at 120 °C for different time: (a) 4 h; (b) 8 h

Hardness (HV) values of aged alloy under different conditions are summarized in Table 4. It can be seen that the hardness of aged alloy increased by increasing the aging time and aging temperature due to the formation of GP zones. The difference percent between the

maximum hardness (HV 187.94) and minimum hardness (HV 161.95) is 16.05%.

Figure 6 shows the tensile properties of the Al–Zn–Mg–Cu alloy aged at different temperatures for various

Table 4 Hardness (HV) of aged alloy

Temperature/ °C	Hardness (HV)			
	2 h	4 h	6 h	8 h
105	161.95	164.46	166.30	167.90
120	164.18	167.27	168.11	180.10.
135	170.89	170.92	173.48	187.94

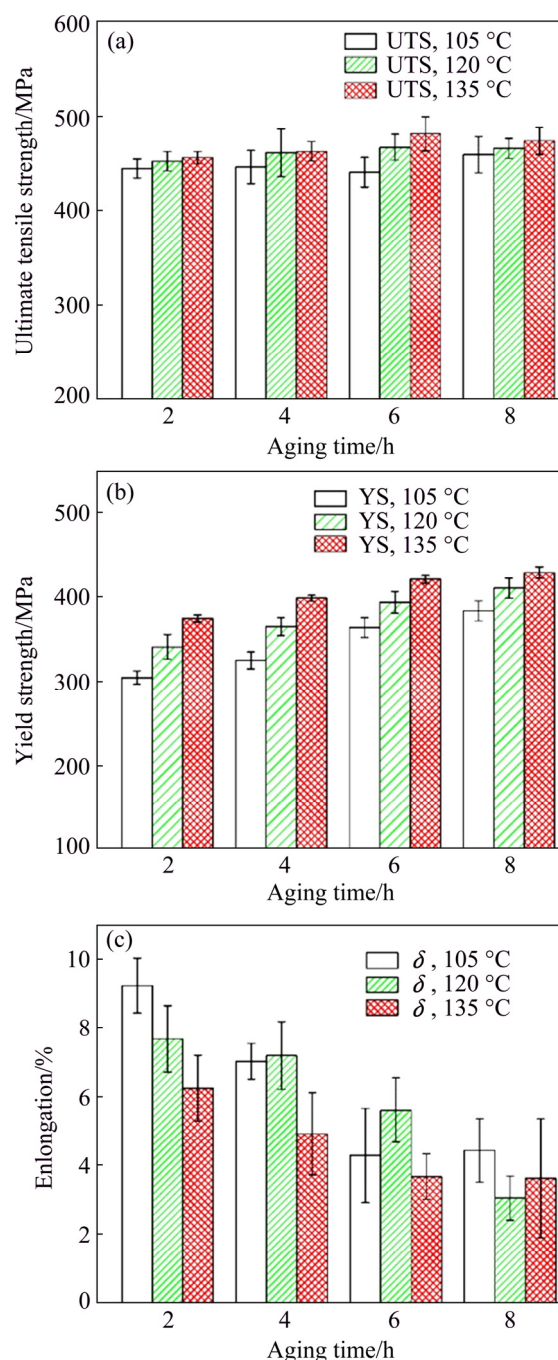


Fig. 6 Tensile properties of under-aged alloy: (a) Ultimate tensile strength; (b) Yield strength; (c) Elongation

time. The results showed that the alloy reached the maximum value of the elongation (δ), and the maximum elongation value was 9.20%, together with a UTS of 444.21 MPa and a YS of 304.57 MPa, when aged at 105 °C for 2 h. This meant that the squeeze-cast Al–Zn–Mg–Cu alloy could obtain excellent ductility and relatively good strength at the same time.

As shown in Fig. 6, the maximum value of UTS of alloy aged under different conditions was 481.04 MPa (135 °C, 6 h) and the maximum value of YS was 428.67 MPa (135 °C, 8 h). However, the value of elongation was less than 5%. Though higher aging temperature and longer aging time could lead to higher strength in this study, the ductility was deteriorated.

Figure 7 shows the fracture images of alloys aged at 120 °C for different time. For under-aged alloy, the dissolution of the solute atoms formed a dispersive distribution of the microscopic GP zones, which resulted in the increase of the strength and the decrease of the ductility. The alloy treated at 120 °C for 2 and 4 h showed the microporous aggregation type ductile fracture, namely dimple type fracture, and the dimples are shown by arrows in Figs. 7(a) and (b). With further increase of aging time, the strength was improved and the ductility was deteriorated. The alloy aged at 120 °C for 6 and 8 h exhibited characteristics of river-shape cleavage fracture, as shown in circles in Figs. 7(c) and (d). The result was consistent with the tensile properties shown in Fig. 6.

The YS of aged alloy is influenced by many kinds of strengthening effects, such as inherent yield strength of aluminum matrix, grain boundary strengthening, solute atoms induced solid solution strengthening, precipitation strengthening effect of precipitated particles and dislocation hardening due to the accumulation of the dislocations. Among them, the precipitation strengthening effect of GP zones is the most important factor. The particle–dislocation interactions, including shearing and bypassing, were considered as the chief strengthening mechanism in aged Al–Zn–Mg–Cu alloy. And most of researchers claimed that the precipitates strengthening mechanism of aged Al–Zn–Mg–Cu alloy is attributed to the strengthening of fine GP zone and metastable η' phase through particle–dislocation shearing mechanism [18].

GP zones in aged Al–Zn–Mg–Cu alloy coherent with aluminum matrix, formed during the early stage of precipitation, can serve as nucleation sites for the heterogeneous nucleation of metastable η' phase which is semi-coherent with the Al matrix. In peak-aged condition, metastable η' phase brings peak strengthening at the expense of the decrease of ductility. In the present study, under-aging process was employed to obtain excellent performance with both high strength and good ductility, and the alloys were strengthened by GP zones instead of metastable η' phase.

Higher aging temperature or longer aging time may lead to the increase of the volume fraction of GP zones,

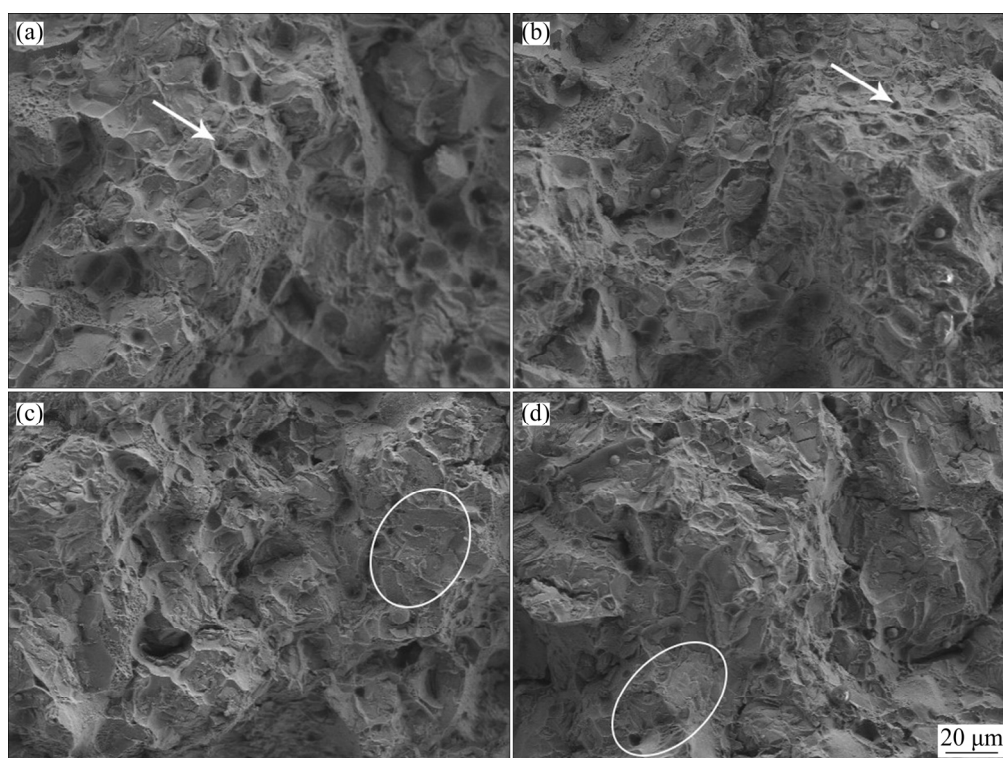


Fig. 7 Fracture images of alloys aged at 120 °C for different time: (a) 2 h; (b) 4 h; (c) 6 h; (d) 8 h

as well as coarsening of the GP zones. The coarsening of GP zones will lead to the decrease of the tensile strength. In the present study, the volume fraction of GP zones increased with the increase of aging time. As the aging time was relatively short, the coarsening of GP zones was not remarkable. Therefore, the yield strength increased with the increase of aging time for the sake of the strengthening effect of GP zones.

The results also showed that the alloys aged at 120 °C for 6 h or at 135 °C for 2 h exhibited a good comprehensive property. Under these two conditions, the values of UTS, YS and δ were higher than 450 MPa, 370 MPa and 5%, respectively.

4 Conclusions

1) The optimal solution process in this study was that the as-cast Al–Zn–Mg–Cu alloy was solution-treated at 470 °C for 4 h. Most of the secondary phases were dissolved under this condition. The elongation of the alloy was greatly improved compared with that of the as-cast alloy. The as-cast alloy showed the intergranular fracture character, while the solution-treated alloy exhibited pure shear fracture.

2) During under-aging process, the supersaturated Al solid solution decomposed, and the precipitation of dispersive microscopic GP zones occurred. The precipitation strengthening of GP zones became the most important factor. Higher aging temperature or longer time aging led to the increase of volume fraction of GP zones and the increase of the strength of the alloys, and the ductility of the alloy was not deteriorated significantly. Thus, the best combination of strength and ductility can be achieved by utilizing appropriate aging temperature and time.

3) The results showed that the alloy reached the maximum value of the elongation, and the maximum elongation value was 9.20%, together with a UTS of 444.21 MPa and a YS of 304.57 MPa, when aged at 105 °C for 2 h. This meant that the squeeze-cast Al–Zn–Mg–Cu alloy could obtain excellent ductility and relatively good strength at the same time. This is a good choice for automotive components with higher ductility requirement.

References

- [1] ZHANG Y, LAI X M, ZHU P, WANG W R. Lightweight design of automobile component using high strength steel based on dent resistance [J]. *Material Design*, 2006, 27: 64–68.
- [2] KASTENSSON A. Developing lightweight concepts in the automotive industry: Taking on the environmental challenge with the SÄNätt project [J]. *Journal of Cleaner Production*, 2014, 66: 337–346.
- [3] LIU J, TAN M, JARFORS A, AUE-U-LAN Y, CASTAGNE S. Formability in AA5083 and AA6061 alloys for light weight applications [J]. *Material Design*, 2010, 31(S): s66–s70.
- [4] KOC M, ALTAN T. An overall review of the tube hydroforming (THF) technology [J]. *Journal of Materials Processing Technology*, 2001, 108: 384–393.
- [5] BAYAZID S M, FARHANGI H, ASGHARZADEH H, RADAN L, GHAHRAMANI A, MIRHAJI A. Effect of cyclic solution treatment on microstructure and mechanical properties of friction stir welded 7075 Al alloy [J]. *Materials Science and Engineering A*, 2016, 649: 293–300.
- [6] GOPALA KRISHNA K, SIVAPRASAD K, VENKATESWARLU K, HARI KUMAR K C. Microstructural evolution and aging behavior of cryorolled Al–4Zn–2Mg alloy [J]. *Materials Science and Engineering A*, 2012, 535: 129–135.
- [7] GHOSH K S, GAO N, STARINK M J. Characterisation of high pressure torsion processed 7150 Al–Zn–Mg–Cu alloy [J]. *Materials Science and Engineering A*, 2012, 552: 164–171.
- [8] SU J Q, NELSON T W, MISHRA R, MAHONEY M. Microstructural investigation of friction stir welded 7050-T651 aluminium [J]. *Acta Materialia*, 2003, 51: 713–729.
- [9] HAN Z Q, HUANG X R, LUO A. A quantitative model for describing crystal nucleation in pressurized solidification during squeeze casting [J]. *Scripta Materialia*, 2012, 66: 215–218.
- [10] KIM S W, KIM D Y, KIM W G, WOO K D. The study on characteristics of heat treatment of the direct squeeze cast 7075 wrought Al alloy [J]. *Materials Science and Engineering A*, 2001, 305: 721–726.
- [11] FAN C H, CHEN Z H, HE W Q, CHEN J H, CHEN D. Effects of the casting temperature on microstructure and mechanical properties of the squeeze-cast Al–Zn–Mg–Cu alloy [J]. *Journal of Alloys and Compounds*, 2010, 504: L42–L45.
- [12] HAN G M, HAN Z Q, LUO A A. Microstructure characteristics and effect of aging process on the mechanical properties of squeeze-cast AZ91 alloy [J]. *Journal of Alloys and Compounds*, 2015, 641: 56–63.
- [13] HAN Z Q, HAN G M, LUO A A. Large-scale three-dimensional phase-field simulation of multi-variant beta-Mg17Al12 in Mg–Al-based alloys [J]. *Computational Materials Science*, 2015, 101: 248–254.
- [14] YANG R X, LIU Z Y, YING P Y, LI J L. Multistage-aging process effect on formation of GP zones and mechanical properties in Al–Zn–Mg–Cu alloy [J]. *Transactions of Nonferrous Metals Society of China*, 2016, 26: 1183–1190.
- [15] FAN X, JIANG D, MENG Q, ZHANG B, WANG T. Evolution of eutectic structures in Al–Zn–Mg–Cu alloys during heat treatment [J]. *Transactions of Nonferrous Metals Society of China*, 2006, 16: 577–581.
- [16] STARINK M J, WANG S C. A model for the yield strength of overaged Al–Zn–Mg–Cu alloys [J]. *Acta Materialia*, 2003, 51: 5131–5150.
- [17] LI H Y, LIU J J, YU W C, ZHAO H, LI D W. Microstructure evolution of Al–Zn–Mg–Cu alloy during non-linear cooling process [J]. *Transactions of Nonferrous Metals Society of China*, 2016, 26: 1191–1200.
- [18] ZHANG Y H, YANG S C, JI H Z. Microstructure evolution in cooling process of Al–Zn–Mg–Cu alloy and kinetics description [J]. *Transactions of Nonferrous Metals Society of China*, 2012, 22: 2087–2091.

欠时效处理对挤压铸造 Al-Zn-Mg-Cu 合金 显微组织及力学性能的影响

王非凡^{1,2}, 孟文^{1,2}, 张宏伟¹, 韩志强^{1,2}

1. 清华大学 材料学院, 北京 100084;

2. 清华大学 先进成形制造教育部重点实验室, 北京 100084

摘 要: 采用光学显微镜、X 射线衍射技术、扫描电镜、透射电镜以及硬度和拉伸试验研究欠时效处理对挤压铸造 Al-Zn-Mg-Cu 合金显微组织及力学性能的影响。结果表明, 在 470 °C、4 h 的固溶条件下, 绝大部分二次相溶解到 $\alpha(\text{Al})$ 基体中, 且枝晶未出现明显的长大。在欠时效工艺条件下, 由于 GP 区的强化效应, 随着时效时间和时效温度的增加, 合金的抗拉强度和屈服强度增加, 而伸长率下降。因此, 可通过控制时效时间和时效温度获得具有较高强度和伸长率的合金, 使汽车零部件性能达到设计要求。

关键词: Al-Zn-Mg-Cu 合金; 挤压铸造; 欠时效处理; GP 区; 沉淀强化

(Edited by Wei-ping CHEN)